EXOTIC NUCLEAR STRUCTURE PHENOMENA IN MEDIUM MASS NUCLEI

O. RADU[1], A. PETROVICI[1,2], K.W. SCHMID[2], A. FAESSLER[2]

[1] Horia Hulubei National Institute for Physics and Nuclear Engineering, Bucharest,Romania
2 Institut für Theoretische Physik, Universität Tübingen, Germany

- shape coexistence effects in ^{78}Kr
- magnetic bands in ^{82}Rb

within
the *complex EXCITED VAMPIR approach*

Variational approaches

to the nuclear many-body problem

using symmetry-projected Hartree-Fock-Bogoliubov configurations

General theoretical tools

- the model space is defined by a finite set of spherical single particle states
- the effective many-body Hamiltonian is represented as a sum of one- and two-body terms
- the basic building blocks are HFB vacua, only restricted by time-reversal and axial symmetry
- the HFB transformations are essentially *complex* and allow proton-neutron and parity mixing
- the broken symmetries are restored by projection techniques ($s = N, Z, I, \pi$)

Model space

$$\{|i\rangle \equiv |\tau n l j m\rangle\}$$

$$\{c_i^\dagger, c_k^\dagger, \ldots\}_M$$

$$\{c_i, c_k, \ldots\}_M$$

Effective many-body Hamiltonian

$$\hat{H} = \sum_{i=1}^{M} \varepsilon(i) c_i^\dagger c_i + \frac{1}{4} \sum_{i,k,r,s=1}^{M} v(ikrs) c_i^\dagger c_k^\dagger c_s c_r$$

Hartree-Fock-Bogoliubov transformation

$$\begin{pmatrix} a^\dagger \\ a \end{pmatrix} = \begin{pmatrix} A^T & B^T \\ B^\dagger & A^\dagger \end{pmatrix} \begin{pmatrix} c^\dagger \\ c \end{pmatrix} \equiv F \begin{pmatrix} c^\dagger_{nlj\tau_z;m\pi} \\ \vdots \\ c_{nlj\tau_z;m\pi} \end{pmatrix}$$

Quasi-particle vacuum

$$|F\rangle = \prod_{\alpha=1}^{M'} a_\alpha|0\rangle \qquad \text{with} \quad \left\{ \begin{array}{ll} a_\alpha|0\rangle \neq 0 & \text{for } \alpha = 1, \ldots, M' \leq M \\ a_\alpha|0\rangle = 0 & \text{else} \end{array} \right\}$$

$$\hat{\Theta}^{s}_{MK} \equiv \hat{P}(I;MK)\hat{Q}(N)\hat{Q}(Z)\hat{p}(\pi)$$

$$\hat{p}(\pi) \equiv \frac{1}{2}\left(1 + \pi\hat{\Pi}\right)$$

$$\hat{Q}(N_\tau) \equiv \frac{1}{2\pi}\int_0^{2\pi} d\phi_\tau \exp\{i\phi_\tau(N_\tau - \hat{N}_\tau)\})$$

$$\hat{P}(I;MK) \equiv \frac{2I+1}{8\pi^2}\int d\Omega D^{I}_{MK}{}^{*}(\Omega)\hat{R}(\Omega)$$

$$|\psi(F^s);sM\rangle = \sum_{K=-I}^{+I} \hat{\Theta}^{s}_{MK}|F^s\rangle\, f^s_K$$

$$|\psi(F^s);sM\rangle = \frac{\hat{\Theta}^{s}_{M0}|F^s\rangle}{\sqrt{\langle F^s|\hat{\Theta}^{s}_{00}|F^s\rangle}}$$

Variational procedures

complex Vampir approach

$$E^s[F_1^s] = \frac{\langle F_1^s | \hat{H} \hat{\Theta}^s_{00} | F_1^s \rangle}{\langle F_1^s | \hat{\Theta}^s_{00} | F_1^s \rangle}$$

$$|\psi(F_1^s); sM\rangle = \frac{\hat{\Theta}^s_{M0} | F_1^s \rangle}{\sqrt{\langle F_1^s | \hat{\Theta}^s_{00} | F_1^s \rangle}}$$

complex Excited Vampir approach

$$|\psi(F_2^s); sM\rangle = \hat{\Theta}^s_{M0} \left\{ |F_1^s\rangle \alpha_1^2 + |F_2^s\rangle \alpha_2^2 \right\}$$

$$|\psi(F_i^s); sM\rangle = \hat{\Theta}^s_{M0} \sum_{j=1}^{i} |F_j^s\rangle \, \alpha_j^i \qquad \text{for} \quad i = 1, \ldots, n$$

$$|\Psi_\alpha^{(n)}; sM > = \sum_{i=1}^{n} |\psi_i; sM > f_{i\alpha}^{(n)}, \qquad \alpha = 1, \ldots, n$$

$$(H - E^{(n)} N) f^n = 0$$

$$(f^{(n)})^+ N f^{(n)} = 1$$

A= 50 – 90 mass region

^{40}Ca - core

model space (π, ν):

$1p_{1/2}\ 1p_{3/2}\ 0f_{5/2}\ 0f_{7/2}\ 1d_{5/2}\ 0g_{9/2}$

renormalized G–matrix (OBEP, Bonn A)

- short range Gaussians in the *nn, pp, np channels*
- monopole shifts:

$$\langle 0g_{9/2}0f; T=0|\hat{G}|0g_{9/2}0f; T=0\rangle$$

$$\langle 1p1d_{5/2}; T=0|\hat{G}|1p1d_{5/2}; T=0\rangle$$

Shape coexistence effects in ^{78}Kr

Nucl. Phys. A770 (2006) 107
J. Phys. G: Nucl.Part.Phys.32(2006) 583

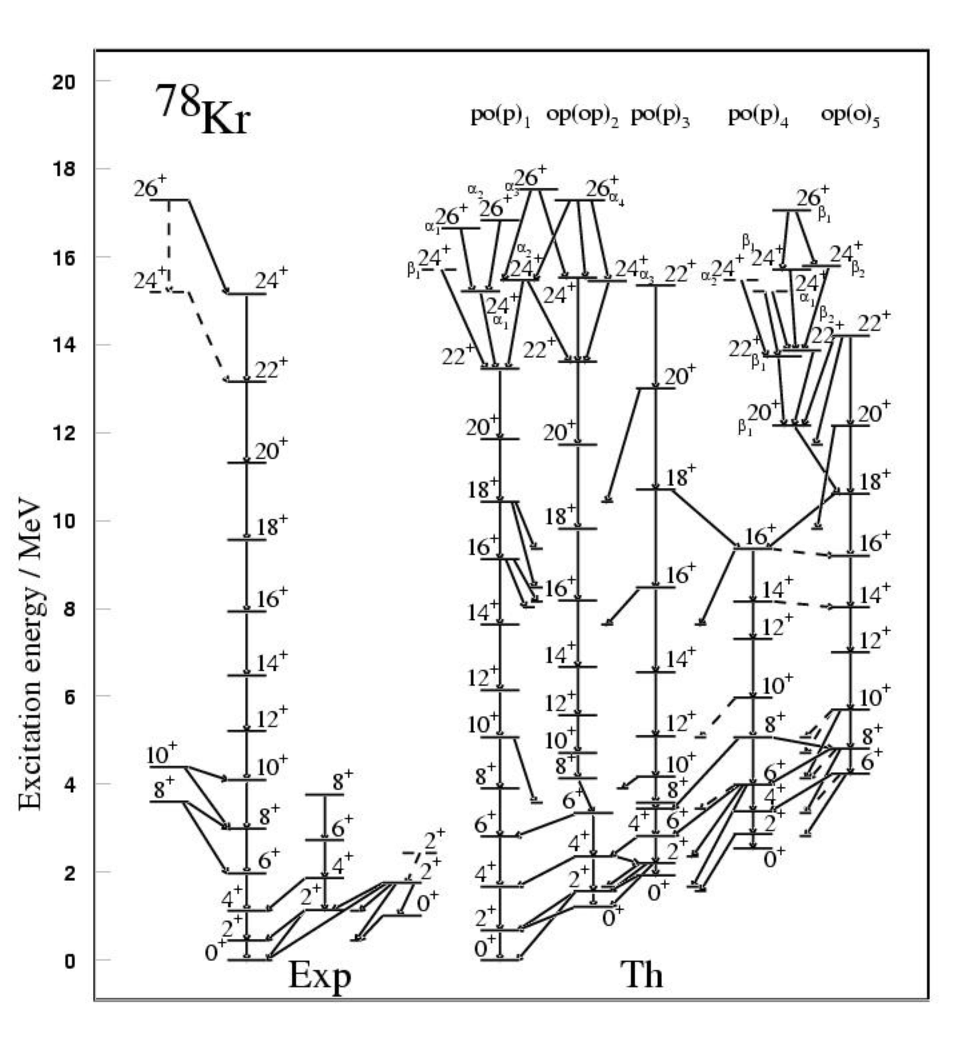

Table 1. The dominant components of the different states of ^{78}Kr.

$I[\hbar]$	o-mixing	p-mixing
0_1^+	13(4)(3)%	74(4)(2)%
0_2^+	51(8)(3)%	24(11)(2)%
0_3^+	22(2)%	75%
0_4^+	18(3)%	61(10)(6)%
2_1^+	5%	88(3)(2)%
2_2^+	82(4)(3)%	8(2)%
2_3^+	5%	91(2)%
2_4^+	4%	72(13)(7)%
4_1^+	3%	88(7)%
4_2^+	91(2)%	5%
4_3^+		88(6)(2)%
4_4^+	2%	74(9)(7)(6)%
6_1^+	2%	64(31)%
6_2^+	92(3)%	3%
6_3^+		51(27)(16)(3)%
6_4^+	2%	60(13)(13)(5)(4)(2)%
6_5^+	53(2)(2)(2)%	21(14)(2)%
8_1^+		50(42)(5)%
8_2^+	71(14)(8)(5)%	
8_3^+		48(31)(11)(7)%
8_4^+	2%	75(8)(7)(4)(2)%
8_5^+	71(19)(4)(2)%	2%
10_1^+		82(7)(5)(2)(2)%
10_2^+	82(7)(4)(4)(2)%	
10_3^+		87(9)(2)%
10_4^+		79(10)(4)(3)(2)%
10_5^+	77(10)(9)(4)%	
12_1^+		82(15)(2)%
12_2^+	94(5)%	
12_3^+		82(14)(2)%
12_4^+		72(22)(2)(2)%
12_5^+	96(3)%	
14_1^+		70(20)(9)%
14_2^+	95(3)%	
14_3^+		69(18)(12)%
14_4^+	3%	74(15)(4)(3)%
14_5^+	93(2)%	2%

$I[\hbar]$	o-mixing	p-mixing
16_1^+	7%	56(27)(6)(2)%
16_2^+	97(2)%	
16_3^+		81(17)%
16_4^+	3(2)%	43(36)(10)(3)%
16_5^+	83(5)(2)%	6(2)(1)%
18_1^+		70(12)(7)(3)(3)(3)%
18_2^+	94(5)%	
18_3^+	6(2)%	66(11)(7)(3)(2)%
18_5^+	84(4)(3)(2)(2)%	3(2)%
20_1^+	3%	80(5)(3)(2)(2)(2)%
20_2^+	85(9)(2)(2)(2)%	
20_3^+		68(19)(6)(4)%
20_5^+	79(7)(3)(2)%	6%
$20_{\beta_1}^+$	9(4)(4)%	70(8)%
22_1^+	4(2)%	51(20)(12)(7)(2)%
22_2^+	85(5)(4)(3)%	
22_3^+		96(2)%
22_5^+	88(3)%	6%
$22_{\beta_1}^+$		38(26)(15)(12)(5)(3)%
$22_{\beta_2}^+$		40(31)(12)(8)(4)%
24_2^+	54(15)(2)%	17(6)(2)%
$24_{\alpha_1}^+$	20(5)(2)(2)%	67(2)%
$24_{\alpha_2}^+$	25(2)%	47(19)(3)(2)%
$24_{\alpha_3}^+$	73(15)(4)(2)%	2%
$24_{\beta_1}^+$		46(28)(22)%
$24_{\beta_2}^+$		47(42)(9)%
$26_{\alpha_1}^+$	40(5)(2)%	48(3)(2)%
$26_{\alpha_2}^+$	47(7)(7)(3)(2)%	30(2)(2)%
$26_{\alpha_3}^+$	2%	93(2)%
$26_{\alpha_4}^+$	79(12)%	4(2)%
$26_{\beta_1}^+$		94(4)%

Table 2. $B(E2; I \to I-2)$ values (in $e^2 fm^4$) for some states of the nucleus ^{78}Kr.

$I[\hbar]$	exp	exp	$po(p)_1$	$op(op)_2$	$po(p)_3$	$po(p)_4$	$op(o)_5$
2^+	1210 (80)		1170 58$op(op)_2$	1066 118$po(p)_3$ 47$po(p)_1$	1201 70$op(op)_2$	1186 [192]	
4^+	1740 (140)	1150 (160)	1806 27$po(p)_3$	1849 38$po(p)_3$	1722 [19]$op(op)_2$	1907	
6^+	2020 (340)	810 (220)	1908 [97]$po(p)_3$	1945 [123]	1095 [462][79] [48]$po(p)_4$	832 549$po(p)_3$ 60$po(p)_1$ 46$op(op)_2$ [277]	480$po(p)_4$ 123$po(p)_3$ 44$op(op)$ [630][291] [126][89]
8^+	1940 (300)	2970 (990)	1881 124$po(p)_4$	1228 [440]$op(o)_5$ [252]	1506 [162]$po(p)_4$	1413 194$po(p)_3$ [331]	798 912$op(op)_2$ 90$po(p)_4$ [288]
10^+	1400 (300)		1728 163$po(p)_3$ [71]$po(p)_4$	1774 [157]	1543 131$po(p)_1$	1320 65$po(p)_1$ [171][144]	1368 254$op(op)_2$ [80]
12^+	1920 (1300)		1714	2025	1632	640[650] [150][135]	2007
14^+			402 [1352]	2104	1550	1572	1800
16^+			1009 168$op(o)_5$ 124$po(p)_4$ [162]	2056	1135 265$po(p)_1$ [170]	1152 140$po(p)_1$ [115]	1695
18^+			809 214$po(p)_4$ 131$po(p)_3$	2066	1038 226$po(p)_4$ [252]		1169 182$po(p)_4$ [180]
20^+			976	1726	644 91$po(p)_1$ [354][225][103]		1268 200$op(op)_2$ [135]
22^+			692 [115][97]	994 [364][101]	1056 [347]		1201 384$op(op)_2$ 142β_1
24^+				714 [97][50]			

Exp

$Q(2^+_1)$= -61(3) efm^2

$Q(2^+_2)$= +44(6) efm^2

Table 4. Spectroscopic quadrupole moments Q_2^{sp} (in efm^2).

$I[\hbar]$	$po(p)_1$	$op(op)_2$	$po(p)_3$	$po(p)_4$	$op(o)_5$
2^+	-61.38	55.23	-63.27	-67.61	
4^+	-84.48	84.34	-87.53	-89.52	
6^+	-96.36	99.02	-95.35	-95.73	22.32
8^+	-101.50	109.36	-100.74	-97.61	99.72
10^+	-101.05	111.28	-105.42	-103.61	105.78
12^+	-98.43	115.11	-107.89	-101.29	107.19
14^+	-100.45	117.39	-106.58	-97.20	101.24
16^+	-85.77	119.94	-106.73	-90.19	87.36
18^+	-95.26	118.54	-81.34		97.97
20^+	-88.55	108.08	-89.40		94.75
22^+	-74.49	94.34	-82.46		104.34
24^+		33.39			

$I[\hbar]$	α_1	α_2	α_3	α_4	β_1	β_2
20^+					-58.41	
22^+					-89.28	-82.46
24^+	-35.02	-38.69	26.46		-80.86	-80.48
26^+	-13.40	12.70	-70.65	64.06	-73.30	

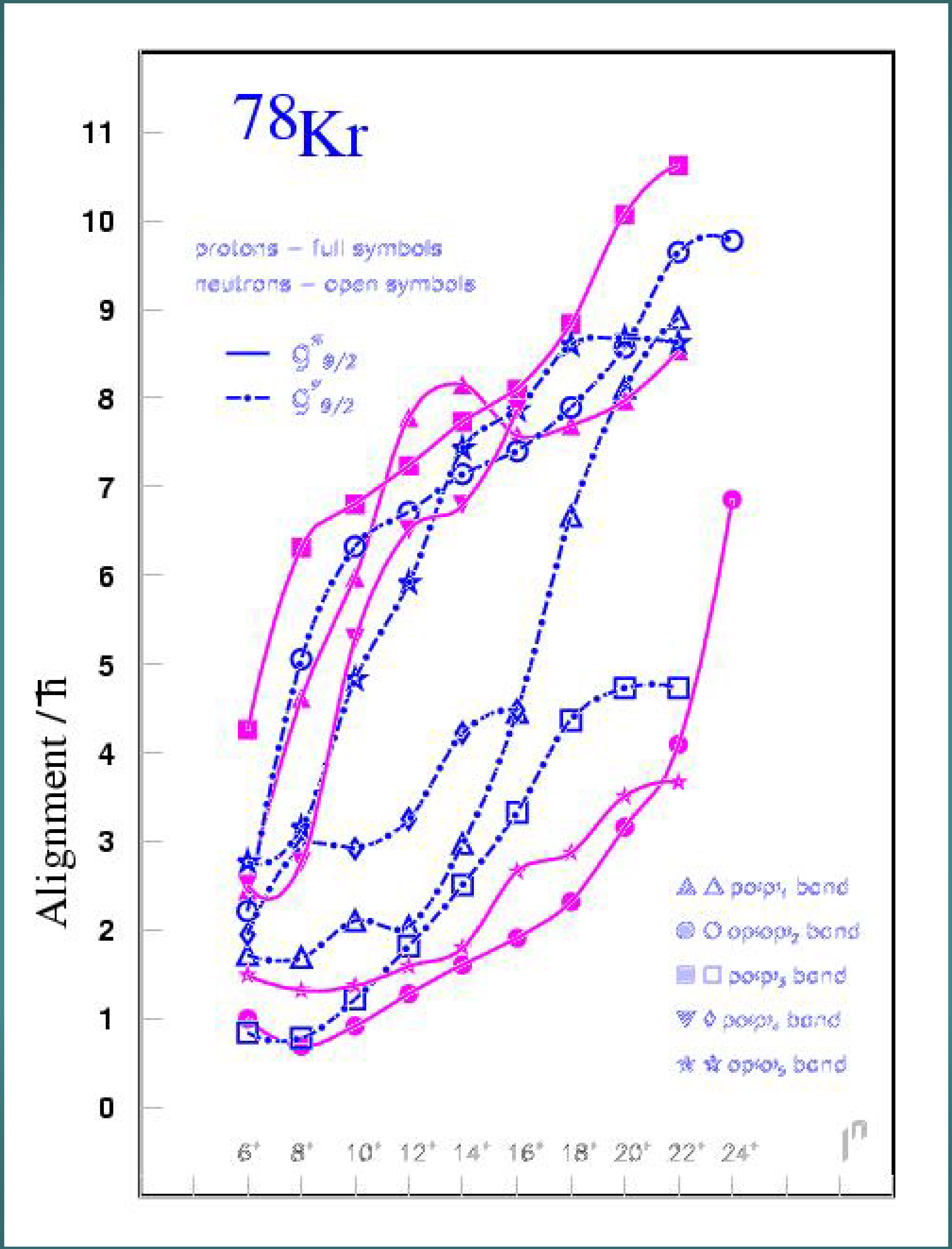
78Kr
Alignment /ħ
protons – full symbols
neutrons – open symbols
0
1
2
3
4
5
6
7
8
9
10
11
6+
8+
10+
12+
14+
16+
18+
20+
22+
24+

Exp.

$g(2^+_1)=0.43(3)$

$g(2^+_2)=0.54(10)$

$g(4^+_1)=0.46(7)$

small effective g-factors at spins 8^+, 10^+, 12^+

Table 5. g-factors (in μ_N) for selected states of ^{78}Kr

$I[\hbar]$	$po(p)_1$	$op(op)_2$	$po(p)_3$	$po(p)_4$	$op(o)_5$	
2^+	0.45	0.50	0.55	0.42		
4^+	0.50	0.48	0.61	0.46		
6^+	0.67	0.37	1.08	0.64	0.33	
8^+	0.90	-0.01	1.21	0.54	0.33	
10^+	0.92	-0.02	1.10	0.76	0.20	
12^+	1.01	0.06	0.99	0.83	0.19	
14^+	0.90	0.13	0.91	0.74	0.14	
16^+	0.75	0.18	0.83	0.75	0.22	
18^+	0.63	0.23	0.78		0.24	
20^+	0.56	0.28	0.80		0.30	
22^+	0.55	0.33	0.67		0.31	
24^+		0.44				
$I[\hbar]$	α_1	α_2	α_3	α_4	β_1	β_2
20^+					0.70	
22^+					0.64	0.67
24^+	0.56	0.51	0.45		0.55	0.59
26^+	0.54	0.52	0.57	0.45	0.50	

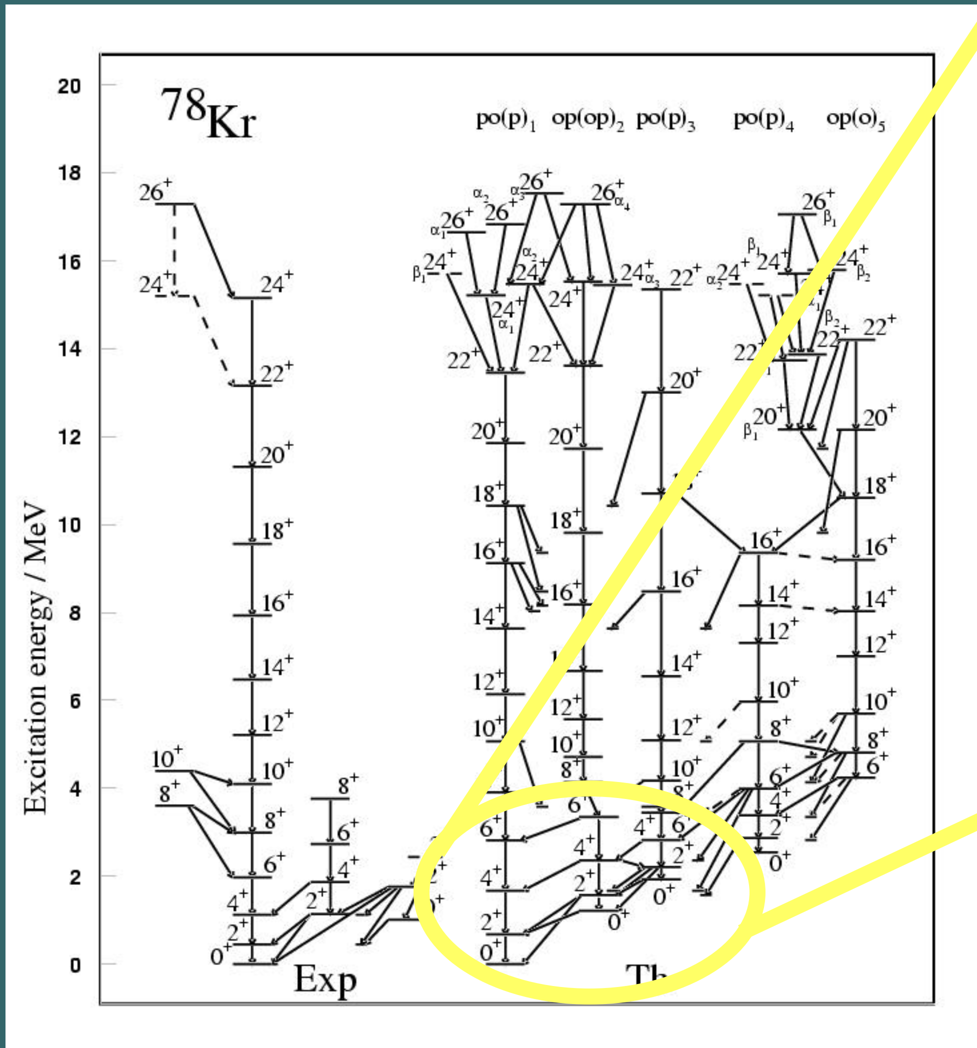

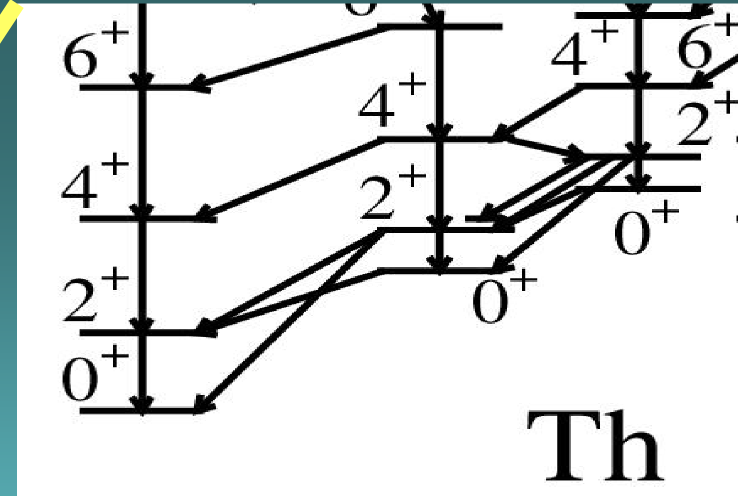

$I[\hbar]$	o-mixing
0_1^+	13(4)(3)%
0_2^+	51(8)(3)%
0_3^+	22(2)%
0_4^+	18(3)%

$\rho^2_{exp}(E0;0^+_2 \to 0^+_1)=0.047(13)$; $\rho^2_{EXV}(E0;0^+_3 \to 0^+_1)=0.017$

Magnetic bands in ^{82}Rb

Eur. Phys. J. A28 (2006) 19

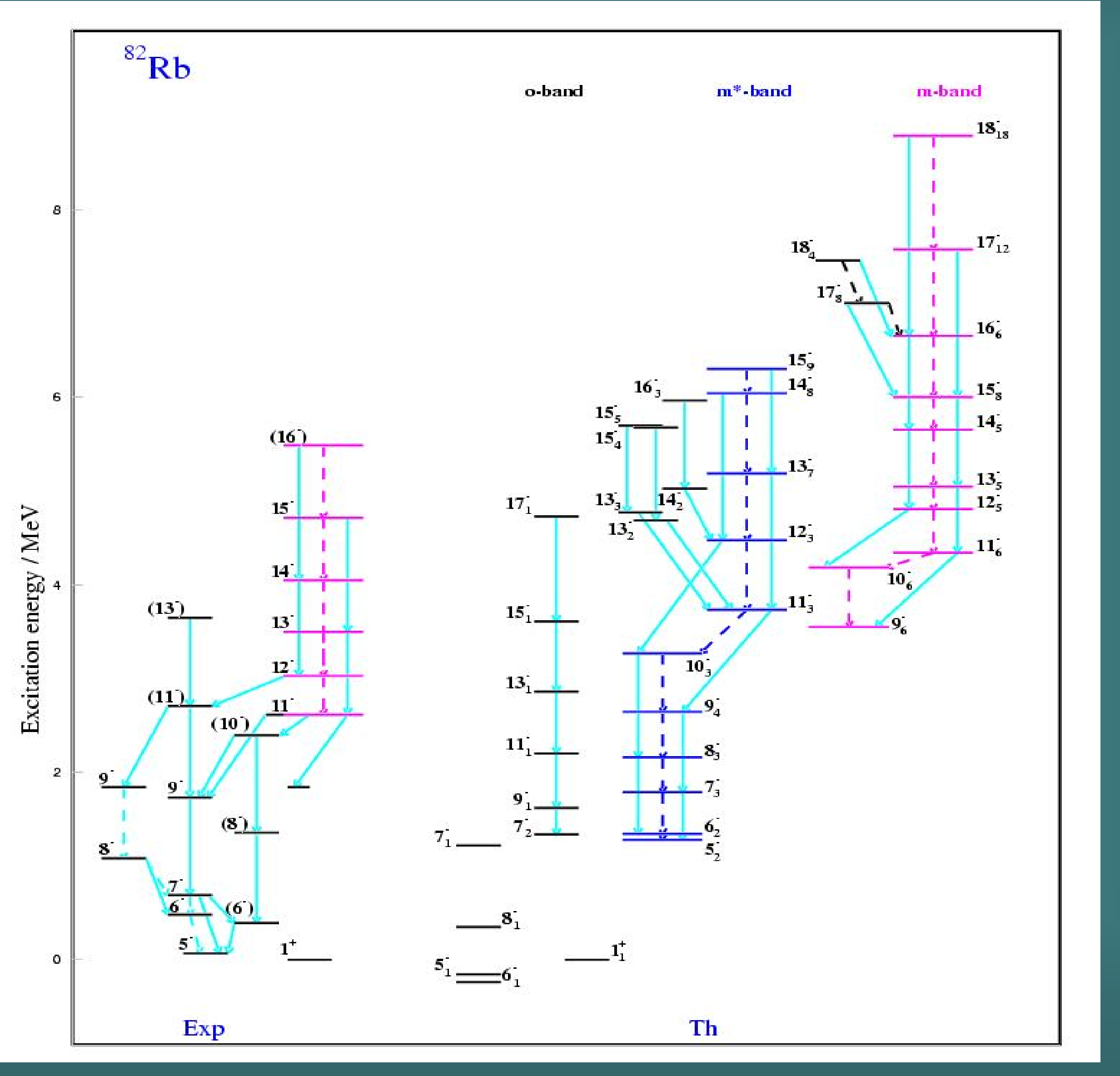

The amount of mixing for some states of ^{82}Rb.

$I^{\pi}[\hbar]$	$m^* - band$ o-mixing	p-mixing	$m - band$ o-mixing	p-mixing
5^-		98%		
6^-		83(12)%		
7^-		97%		
8^-		97%		
9^-		94%		96(3)%
10^-		95%	12(8)(4)%	57(4)(4)%
11^-	3%	87(6)%		90(7)%
12^-	23(10)(7)(3)	47(4)%	4%	59(15)(13)%
13^-	23(11)(4)(3)%	50(4)%	11%	66(19)%
14^-	30(8)(7)(4)%	18(11)(5)(3)(3)%	6%	56(27)(3)%
15^-	44(9)(8)%	27(3)(3)%	5(3)%	62(21)%
16^-			33%	23(30)(7)%
17^-			7(7)(5)(4)%	68(3)%
18^-			8%	54(23)(3)%

$B(E2; I \to I-2)$ values (in e^2fm^4) for some states of the nucleus ^{82}Rb.

$I^\pi[\hbar]$	*Exp*	σ-band	m^*-band	m-band
7^-			815	
8^-			668	
9^-		562	824	
10^-			828	
11^-		516	828	840
12^-			490	196
13^-	384^{+131}_{-106}	424	273	583
14^-	511^{+193}_{-129}		101	487
15^-	>110	436	205	618
16^-				349
17^-		330		302
18^-				66

$B(M1; I \to I-1)$ values (in μ_N^2) for some states of the nucleus ^{82}Rb.

$I^\pi[\hbar]$	*Exp*	m^*--band	m-band
7^-		1.66	
8^-		1.36	
9^-		2.09	
10^-		1.00	0.48
11^-		1.99	1.13
12^-	$1.24^{+0.37}_{-0.24}$	0.35	0.45
13^-	$0.77^{+0.20}_{-0.13}$	0.86	0.86
14^-	$0.74^{+0.22}_{-0.14}$	0.06	0.46
15^-	>0.11	0.26	1.04
16^-			0.40
17^-			0.07
18^-			0.33

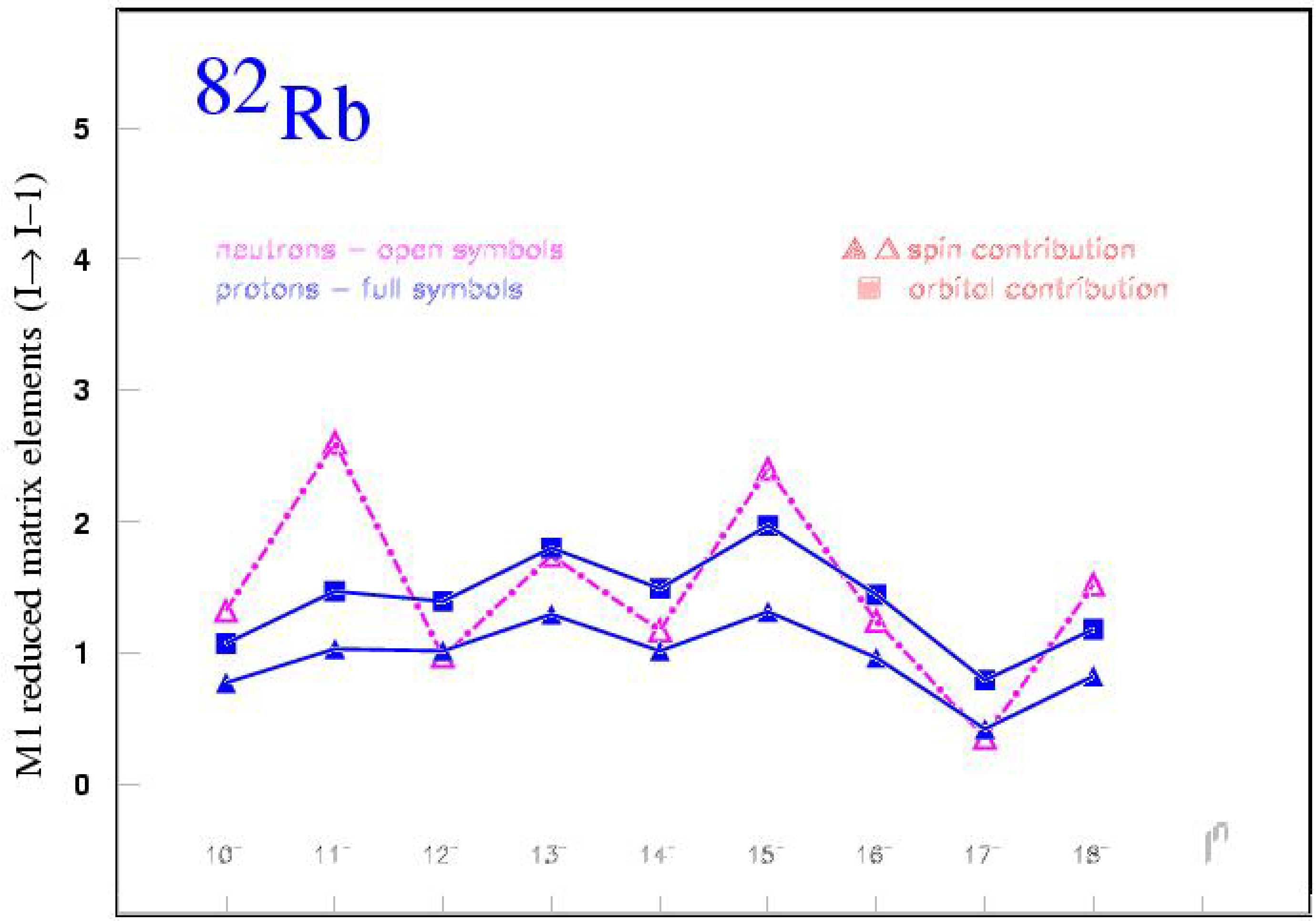

^{82}Rb
M1 reduced matrix elements (I→ I–1)
neutrons – open symbols
protons – full symbols
spin contribution
orbital contribution
5
4
3
2
1
0
10⁻
11⁻
12⁻
13⁻
14⁻
15⁻
16⁻
17⁻
18⁻

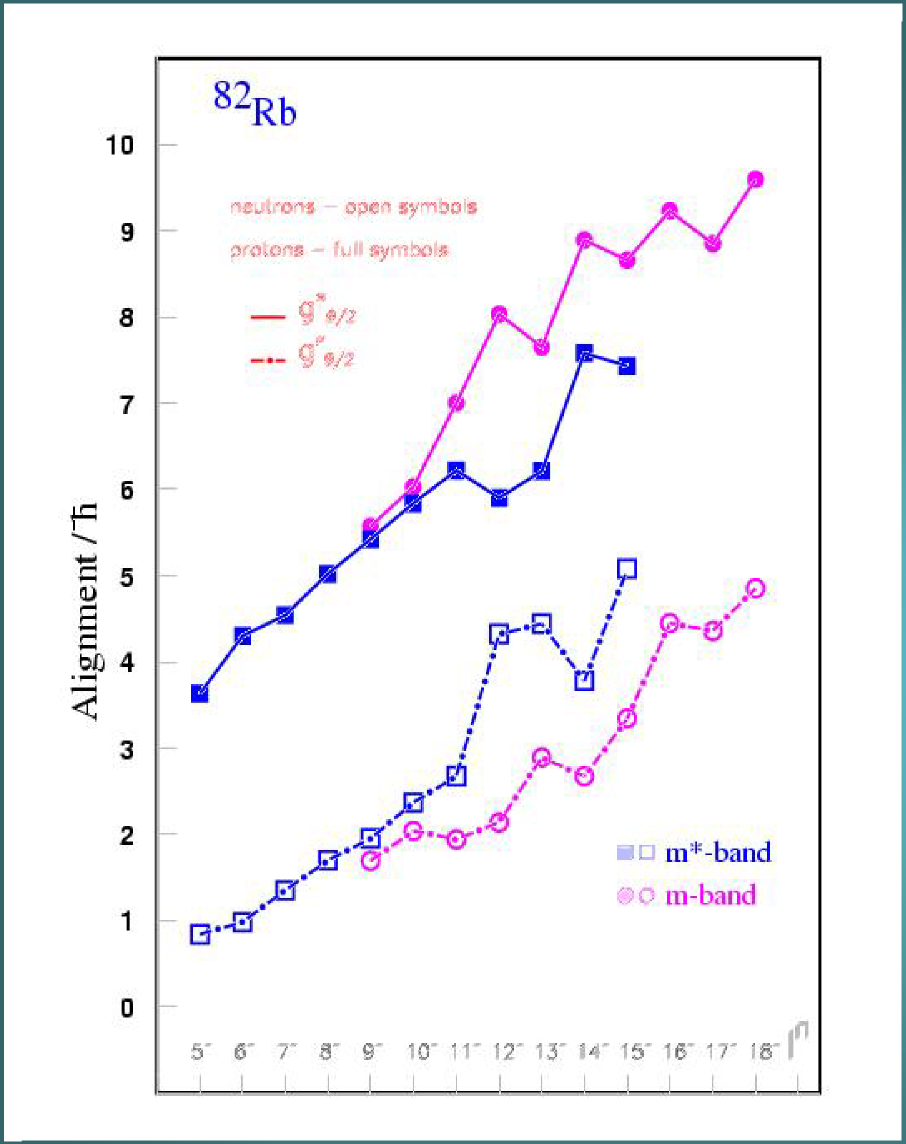

82Rb
neutrons – open symbols
protons – full symbols
g9/2
g9/2
m*-band
m-band
Alignment /ħ
10
9
8
7
6
5
4
3
2
1
0
5⁻ 6⁻ 7⁻ 8⁻ 9⁻ 10⁻ 11⁻ 12⁻ 13⁻ 14⁻ 15⁻ 16⁻ 17⁻ 18⁻
Iπ

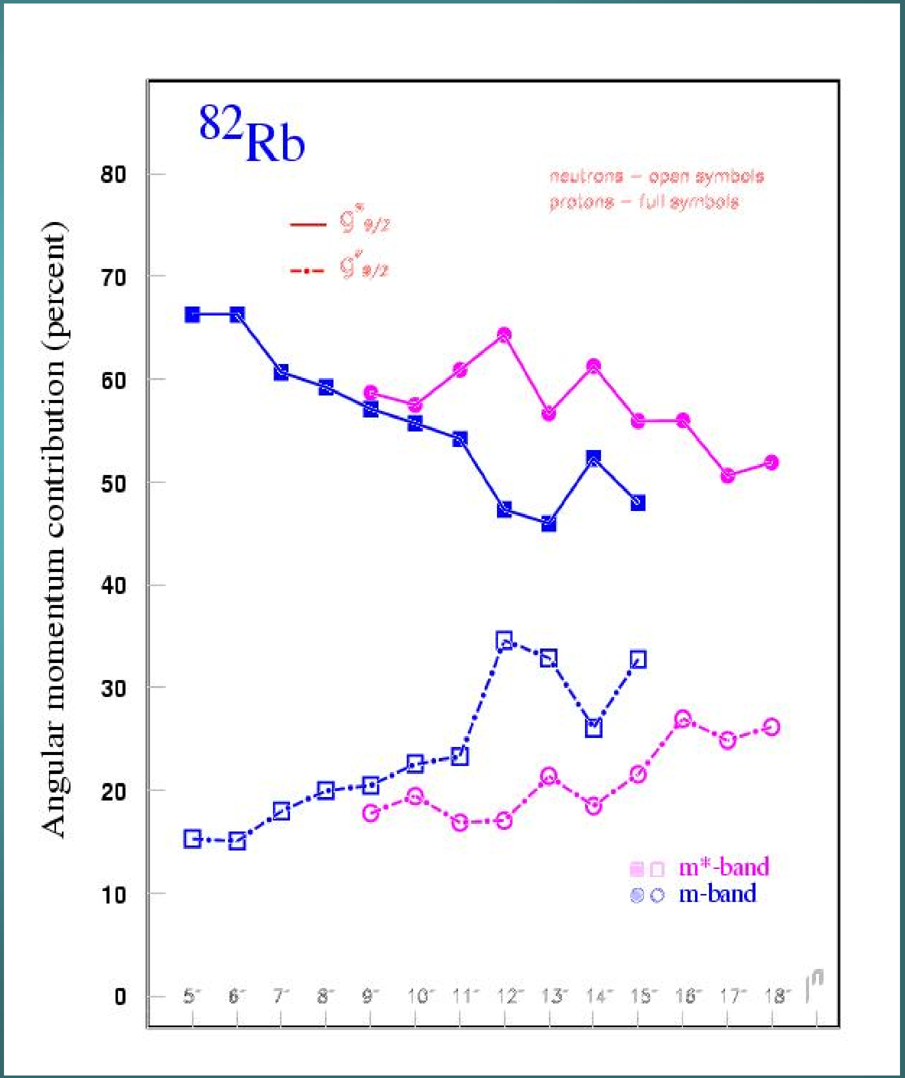

82Rb
neutrons – open symbols
protons – full symbols
g9/2
g9/2
m*-band
m-band
Angular momentum contribution (percent)
80
70
60
50
40
30
20
10
0
5⁻ 6⁻ 7⁻ 8⁻ 9⁻ 10⁻ 11⁻ 12⁻ 13⁻ 14⁻ 15⁻ 16⁻ 17⁻ 18⁻
Iπ

Summary and outlook

• the shape coexistence and the variable oblate-prolate mixing with increasing spin and excitation energy could explain the irregularities observed at low, intermediate and high spins
• the forking observed at the highest identified spins is determined by a high density of strongly mixed configurations
• the calculated electromagnetic properties agree with the available data

• an alternative mechanism to the shears bands able to describe microscopically the phenomenon in the A~80 mass region is provided
• the experimental trend is produced by an increased mixing of differently deformed states at the highest calculated spins

• the description of the exotic phenomena in medium mass nuclei requires very large many-nucleon model spaces

• considerable effort has to be devoted deriving improved effective interaction